# A PERSPECTIVE OF THERMAL TYPE DESALINATION: TECHNOLOGY, CURRENT DEVELOPMENT, AND THERMODYNAMICS ANALYSIS

**Zohreh Rahimi-Ahar** and **Mohammad Sadegh Hatamipour**
*Chemical Engineering Department, University of Isfahan, Isfahan, I.R. Iran*

**Keywords:** thermal desalination, performance ratio, hybrid system, co-generation

**Contents**



**Summary**

An overview is provided, which explores different types of thermal desalination units, focusing on conventional and hybrid desalination technologies that address the global water crisis. Low-cost desalination methods are developed by coupling different thermal-based desalination systems with vapor compression, reverse osmosis or an adsorption cycle. Hybrid systems produce high-quality freshwater and have a cooling effect. Owing to the future global demand for freshwater and power due to the population growth and fast rate of industrial development, dual-purpose power-desalination (co-generating) plants are also studied. The conventional thermal desalination processes and hybrid systems are evaluated from the energy-exergy point of view to evaluate the process efficiency. The effects of the main parameters in different processes on system performance and energy-exergy efficiencies are stated.

## 1. Introduction

The need for drinkable water poses a great problem in arid areas where freshwater is becoming scarce. An increase in the world population combined with industrial and agricultural activities leads to the reduction of freshwater resources. Desalination as one of the primary methods of water treatment is a common solution to overcome water shortage. Desalination uses a great amount of energy to separate pure water from saline water (Qiblawey and Banat, 2008). Desalination plants are classified as shown in Figure 1. Thermal-based desalination is accomplished using multiple-effect distillation (MED), also known as multiple-effect evaporation (MEE), mechanical and thermal vapor compression (MVC and TVC), humidification-dehumidification (HDH), multi-stage flash distillation (MSF), membrane distillation (MD) and solar still (SS) (Alpatova et al, 2018). Power generation, unit capacity, process scheme, and fuel cost affect the selection of the desalination process (Mayor, 2019).

Due to the high energy consumption of desalination processes, numerous investigations have been conducted to decrease the specific energy consumption (SEC), which is the required energy to produce 1 kg of pure water as:

$$SEC = \frac{\dot{m}_{pw}}{\dot{W}_{in}} \quad (1)$$

where, $\dot{m}_{pw}$, and $\dot{W}_{in}$ are desalination rate and required electrical energy for running the electrical devices, respectively (Ayati et al, 2019).

To operate thermal desalination processes, thermal and electrical energies are required. The electrical and thermal energies are essential for running the pumps and evaporating seawater, respectively. Other performance parameters are gained output ratio (GOR), which indicates the thermal energy required to produce 1 kg of desalinated water, and performance ratio (PR), which means the thermal and electrical energies required to produce 1 kg of desalinated water. These items are defined as:

$$GOR = \frac{\dot{m}_{pw} h_{fg}}{\dot{Q}_{in}} \quad (2)$$

$$PR = \frac{\dot{m}_{pw} h_{fg}}{\dot{Q}_{in} + \dot{W}_{in}} \quad (3)$$

where, $\dot{m}_{pw}$, $h_{fg}$, $\dot{Q}_{in}$, and $\dot{W}_{in}$ are desalination rate, latent heat of vaporization, required thermal energy for saline water evaporation, and required electrical energy for operating the electrical devices.

High GOR and PR and low SEC are the specifications of newly designed desalination units (Rahimi-Ahar et al, 2018). Thermal type desalination technologies are tabulated in Table 1 based on the GOR, plant capacity, and maximum process temperature. Improving the efficiency of the components (evaporator, condenser, and pump), using renewable energy sources, and reducing the operation temperature, improves the system performance (Su et al, 2019). For further improvement in the performance, a vacuum evaporator or humidifier based on the hydrostatic head can be used (Choi , 2017; Elsharqawy et al, 2013). The desalination rate increases with the height of the passive vacuum tube with no extra energy consumption for creating the vacuum.

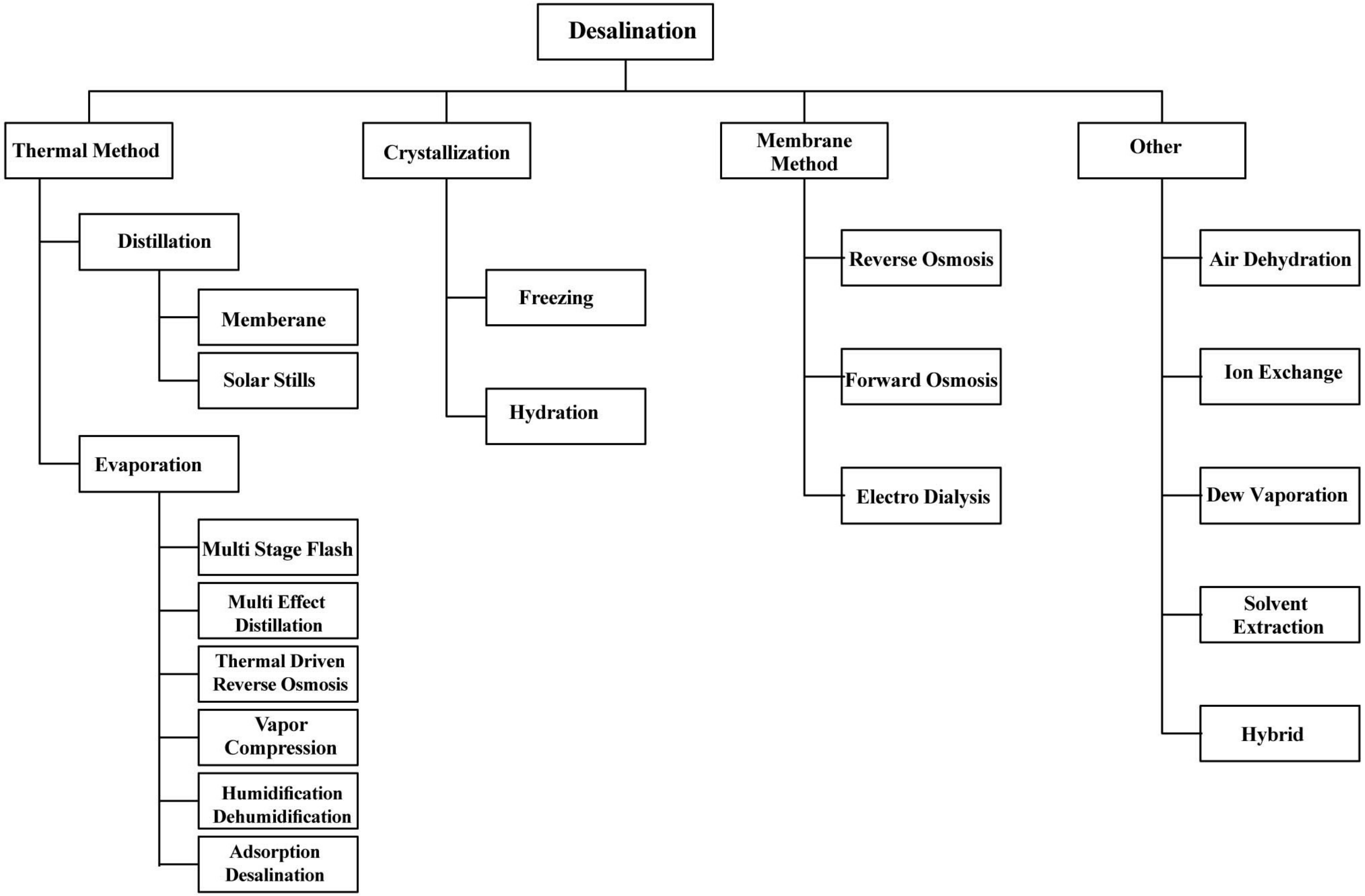


Figure 1. Classification of desalination plants

MED and MSF plants have the benefits of using low-grade heat for evaporation, following the production of desalinated water. In MED, the energy is supplied to the first effect of the unit. The system performance and produced water cost depend on the number of effects. In MSF, the superheated steam is used in the brine heater. The produced top brine temperature (TBT) is in the range of 90-110 °C. The low-grade heat produced from a sulfuric acid plant can be used as the heating source in the MSF and MED plants (Shih, 2005). MSF process has a lower performance ratio (PR) than MED in the waste heat-assisted type systems. This is due to the low temperature at the entrance of the brine heater, which is heated via released low-grade heat source. An economic and technical performance study of the steady state MSF, reverse osmosis (RO), and MSF–RO models revealed that the MSF-RO has lower cost and higher recovery than MSF, and higher water quality than RO (Malik et al, 2016).

| **Desalination method** | **Maximum GOR** | **Capacity ($\times 10^6$ $m^3$/d)** | **Maximum process temperature (°C)** |
|---|---|---|---|
| RO | - | 37 | 45 |
| MSF | 14 | 17 | 115 |
| MED | 25 | 6 | 80 |
| VC | 12-14 | - | 100 |
| HDH | <16.7 | - | 90 |
| MD | - | - | 90 |
| Others (MED-RO, MSF-RO, MD) | - | 12 | 80 |

Table 1. Desalination method and production capacity (IDA, 2016-17; Shih, 2005; Malik et al, 2016; Bundschuh et al, 2015;Pouyfaucon and García-rodríguez, 2018)

It is notable that RO is not recommended for high salinity feed water (above 45000 to 47000 ppm). It is more expensive process due to the frequent maintenance requirement and consuming high-grade energy. Other drawback of RO process are declining fresh water quality over time, inappropriate operation for zero liquid discharge that is environmentally challenging process, passing toxins from membranes and vulnerability of membranes due to biological fouling. Some policies such as pre-treatment operation for the algal removal of saline water (especially gulf waters) and using ultrafiltration membranes are recommended (Villacorte et al, 2014; Ahmadvand et al, 2019 ; Villacorte et al, 2014).

Investigation on the geothermal and solar-based technologies confirms that geothermal technology is superior to the solar-driven processes if low-cost geothermal heat is accessible. This superiority is due to provision of continuous heat in contrast to solar energy (Bundschuh et al, 2015). Furthermore, the geothermal based desalination plants have the potential to be up-scaled, which is not possible with solar. The intermittence of sunshine limits the up scaling in solar desalination technology.

Solar-assisted desalination technologies were investigated by consideration of rural societies with low drinkable water demand; districts with a requirement of both water and electricity, and intermediate drinkable water requirement by Pouyfaucona and García-Rodríguez (2018). Dish concentrator coupled to a micro gas turbine (GT), PV panels used for energy production, while RO, MD, and electrodialysis (ED) desalination processes were recommended for water production in rural communities. Regions with water demands over 25,000 $m^3.d^{-1}$ required solar power plant and RO for energy and water production, respectively. RO driven by parabolic trough collectors (PTCs) or linear Fresnel concentrators could produce the required water for regions with intermediate water production requirements.

One direct solution for performance improvement of desalination processes comes from their hybridization with the newer desalination technologies (adsorption desalination) and power plants (Ng et al, 2015).

An increase in desalinated water demand encourages the researchers in the desalination field to develop modified configurations of conventional desalination processes. Hybrid desalination systems, optimization, desalination-power plants, and thermodynamic analysis are the solutions for improved design. This chapter provides a comprehensive review of various experimental and theoretical advancements carried out for performance improvement of thermal-based desalination processes, focusing on the past and recent ideas. The influence of various effective parameters on the system performance is also discussed.

## 2. Assessment of Recent Developments in Thermal Desalination Systems

### 2.1. Desalination based on Multi-Stage Flash (MSF)

The MSF units involve the largest thermal desalination plants supplying freshwater to many areas, especially in the Middle East and Northern Africa, where thermal desalination still prevails over membrane units. The schematic diagram of the MSF desalination system is presented in Figure 2.

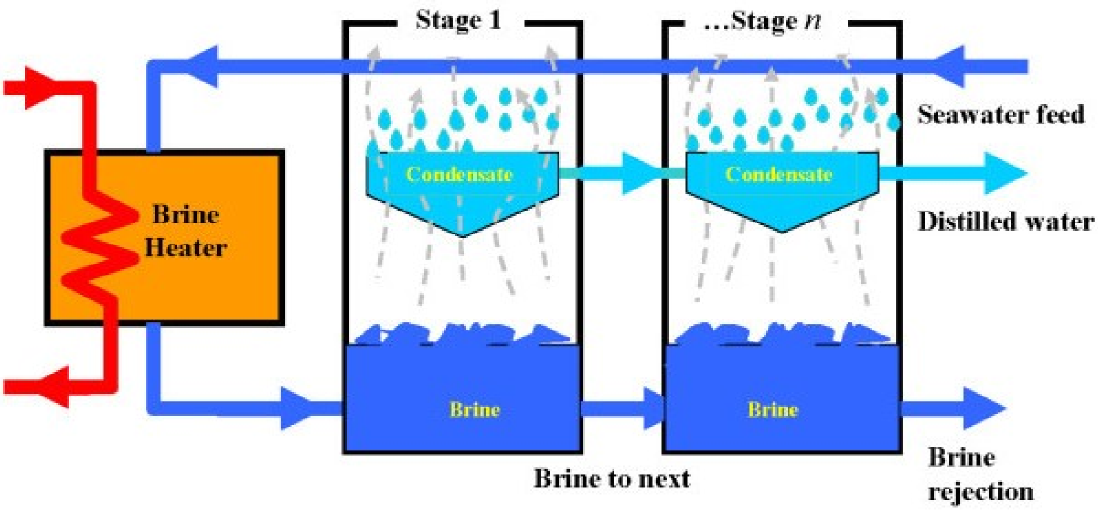


Figure 2. Schematic diagram of multi-stage flash (MSF) desalination system

The feed water is heated by steam in the 1st stage, flows into a series of compartments. The pressure reduces successively in the following stages, and the differential pressure between the stages (driving force for evaporation) builds up. Saline water that has not evaporated in the 1st stage moves into the 2nd stage and the process continues to the last stage. The released vapor condenses giving desalinated water, and at the same time, its condensation enthalpy transfers to the entering feed water. A conventional MSF encompasses brine heating followed with flash distillation in multiple stages to recover the heat. An MSF plant consists of the brine heater, heat rejection, and heat recovery sections. Once through (OT), simple mixer (M) and brine recirculation (BR) designs have been introduced. Among them, OT is the simplest in design, while, the BR design is efficient (Bandi et al, 2016). In MSF-OT design the total brine flows once-through the process, in MSF-M design, part of brine is mixed with incoming saline fed water. In MSF-BR design the processed seawater mixes with the brine leaving the last stage. TBT is one of the main factors that affect the optimum design of MSF. It is a function of boiling point temperature at zero salinity, and temperature elevation owing to salinity. The temperature elevation is predictable by neural-network based correlations (Tanvir and Mujtaba, 2006). MSF performance is enhanced by recovering the sensible heat from the distillate at the MSF stages to increase the temperature of make-up seawater (Al-Weshahi et al, 2014).

Some features of MSF are listed as follows (Compain, 2012):

- High reliability
- No pre-treatment requirement
- High investment cost
- The capability of producing pure water
- Low running flexibility (low variant in flowrate)
- Less scale formation than other thermal desalination methods.

An MSF system with brine extraction and re-injection into flashing chambers technology was developed and was analyzed economically by Al-Hamahmy et al (2016). The extracted brine did not flow into the brine heater or high-temperature flashing stage. Therefore, the surface area of the condenser at the brine heater and the flashing stage was reduced. The condensation heat load is transferred to lower temperature flashing stages, where a cheaper condenser tube material was used. Single-point brine extraction showed better performance than multiple-point brine extraction. It was due to the increase in simplicity and reduction in the robustness of the MSF. The optimum extraction ratio of 9% was resulted and caused a 7.2% enhancement in GOR, a 3.5% decrease in SEC, and a 3.9% reduction in production cost.

The most costly operational problems in thermal desalination processes are scale formation and corrosion in the equipment (Hawaidi and Mujtaba, 2010). A steady-state model of MSF was developed based on the mass and heat balances by consideration of supporting correlations related to physical properties. It was resulted that a 90% increase in the brine heater fouling causes a decrease in the heat transfer coefficient and TBT; hence, the desalination rate reduced by 5.5%. The higher fouling factor led to an increase in steam consumption. The optimization of recycled brine flow rate and steam temperature minimized the operation cost of the MSF that led to the best operation policy for a year.

The SEC evaluation of a MSF (20-stage) plant was reported by Hanshik et al (2016). It was indicated that the performance of the MSF system increases with the elevation of TBT and by varying the operating conditions of the proposed plant. The TBT elevation extended the capacity of MSF, and a large-scale brine rejection pump was required. Replacing a condensate pump solved this problem. The TBT increase caused fouling, and the proper antiscaling materials were required.

The performance of MSF using antiscalants derived from organo-phosphonates, polyelectrolytes, and polyphosphates was studied by Hamed and Al-Otaibi (2010). The antiscalants were examined in an MSF plant at TBT of 119 °C. It was recommended to control the scale formation by optimization of the antiscalant dose rate.

A computational fluid dynamics (CFD) study of the flashing process was developed using two-phase VOF (volume of fluid) formulation by Nigim and Eaton (2017). Two phase-change mechanisms were followed based on the vapor pressure and the saturation temperature. The flow pattern, phase change area, shape of free area, and behavior of the flashing chamber were predicted by solving the steady multi-phase flow equations. Bubble formation was reduced along the length of the flashing chamber. CFD provided a good estimation of the non-equilibrium temperature difference and flashing efficiency.

An MSF plant using two PTCs and a solar pond was simulated via ASPEN HYSYS by Al-Othman et al (2018). The plant was equipped with a boiler to provide the required heat for the process at sunset times. An amount of 1880 $m^3.d^{-1}$ desalinated water was produced out of 40,000 $m^3.d^{-1}$ of seawater. It was shown that PTCs and solar ponds by aperture areas of 3160 $m^2$ and 0.53 $km^2$ provide 76% and 24% of the process energy requirements, respectively.

Multi-stage vacuum chambers of flat plate solar collectors were applied to run a solar MSF unit (Darawsheh et al, 2019). It was found that by 20% pressure reduction in the vacuum flash chamber, the distillation to evaporation ratio and SEC are improved by 53% and 35%, respectively. The solar MSF process enhanced system performance, cost, and energy-saving by increasing vacuum pressure inside the chambers.
A solar-powered MSF plant comprising of two concentrating solar collectors and two storage tanks was investigated by Alsehli et al (2017). The storage tanks received pre-heated brine extracted from the MSF. The brine is heated in collectors to reach the TBT. Operating the dual-tank system provided hot water at all times and preserved TBT from energy losses. By adjusting the mass flow rates, a similar TBT was provided. The system with a collector area of 42,552 $m^2$ resulted in a desalination rate of 2230 $m^3.d^{-1}$ with a total water price of \$2.72/ $m^3$.

An MSF producing 20 MIGD (million imperial gallons per day) of desalinated water was studied by Mabrouk (2013). The brine recycled MSF with long and cross tube bundle evaporators were used. The heat transfer area of the long tube was 25% lower than that of the cross tube, due to the improvement in the heat transfer rate and less energy consumption of the pump used in the long tube design. Condensation was enhanced by using five long tube bundles per each stage.

## 2.2. Desalination based on Multiple Effect Process

MED (or MEE) is used for small/medium scale (2,000 to 15,000 $m^3.d^{-1}$) to large-scale (up to 25,000 $m^3.d^{-1}$) plants. Contrary to MSF, MED uses water at low temperature or vapor. It is comprised of a series of chambers in which the latent heat is used for evaporation. The generated vapor in the 1st stage flows to the 2nd stage and is used to evaporate part of the feed water coming from the 1st stage. The produced vapor flows to the 3rd stage, at a lower pressure than the previous stages. This proceeds up to the last stage, where the vapor is directed to the condenser (Messineo and Marchese, 2008). The schematic diagram of the MED desalination system is presented in Figure 3. Coupling MED with the VC process decreases running costs while increases the unit capacity and heat transfer coefficient.

Some features of MED are as follows (Compain, 2012):
- Easy start-up;
- The capability of producing high-grade freshwater;
- Operation by a low-temperature heat source (prevention of scale formation and corrosion);
- No necessity to pre-treating due to very low scaling;
- Adaptability to co-generation.

A forward feed multi-effect evaporation (FF-MEE) desalination plant, using solar (flat-plate collector) and wind (wind turbine) sources, was simulated by Halil and Söylemez (2012). In FF-MEE the brine and the distillate flowed through successive effects in the pressure and temperature reduction routes (1st to the last effect), while the feed seawater flows in the opposite direction. The thermodynamic laws and the mass-heat balance equations were applied. It was found that the solar energy is more stable than wind energy due to the fluctuation of wind velocity during the operation.

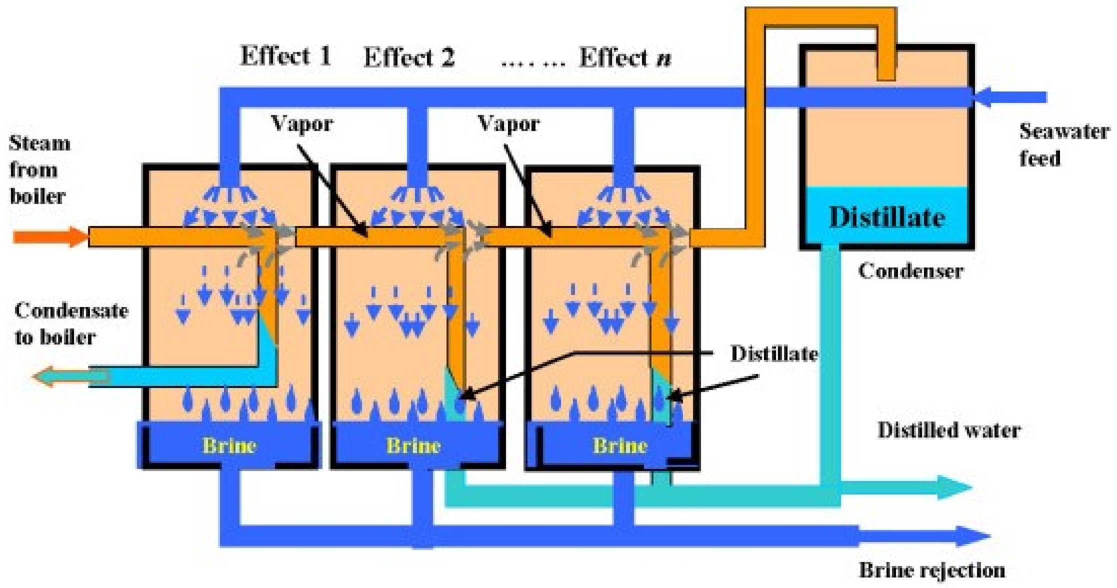


Figure 3. Schematic diagram of multi-effect distillation (MED) desalination system

A six-effect MEE system was simulated and optimized at a steady-state condition by Khademi et al (2009). Among condenser pressure, feed flow rate and feed temperature, the feed temperature played the most important role in the MEE output. The feed flow rate of 51,408 $kg.h^{-1}$ and condenser pressure of 7.6 kPa were the optimized values.

A concentrating PV/thermal collector field coupled to an MEE plant was simulated by Mittelman et al (2009). The proposed dual-purpose system produced water and solar electricity, simultaneously. The cost of produced water in the coupled system was compared with stand-alone MEE and RO. It was found that the coupled system is more cost-effective than the solar MEE approach. RO running by a PV was the best solar alternative where solar desalination plants were more costly than the conventional ones.

The prospects for a 6-effect MEE process improvement were investigated through the thermo-economics aided optimization using pinch-based technique (Piacentino and Cardona, 2010). The optimization of the MEE system involved solving the non-linear equations of mass and heat balances for the evaluation of phase equilibria, heat transfer rate, thermodynamic and chemical properties. It was shown that the flash at brine inlet and the exergy loss at the pre-heaters cause high exergy destruction when the temperature difference between two successive effects increases. The proposed technique revealed the limitations of the integration of cogeneration and desalination systems. It was due to the heat supply that depended on the cost of steam, fuel, and electricity.

A low-temperature MEE plant containing horizontal-tube falling film evaporator was investigated thermodynamically (Shen et al, 2018). It was shown that the distribution of temperature is not uniform in the tube bundle. This non-uniformity of the temperature distribution should be considered in the evaluation of the heat transfer rate.

Four arrangements of MED including backward feed (BF), forward feed (FF), parallel feed (PF) and parallel/cross feed (P/CF) were modeled in steady and unsteady operations by Elsayed et al (2018a). A TVC was coupled to the last effect of P/CF configuration and was compared with the other configurations regarding GOR and SEC to prove the benefit of this integration. TVC-P/CF achieved the lowest produced water cost. Unsteady state modeling showed that TVC-P/CF has the fastest response to the applied disturbances. Variation in parameters led to the highest variation in GOR for the MED-TVC process in comparison with the BF, FF, and P/CF type MEDs. A reliable control could avoid operational disturbance. It was proved that the P/CF has the best performance characteristics among all feed configurations regarding GOR and SEC. The highest exergy destruction of 58% occurred within the TVC that could be reduced by decreasing the motive steam pressure. The exergy destructions related to the pumps and condenser were in the range of 4 to 6.7% of overall exergy destruction (Elsayed et al, 2018b).

The efficiency of an MED operated with thermocline energy from the sea was proposed by Shahzad et al (2018). MED performed well at the temperature difference of 20 °C that was created between the warm surface and cold sub-surface water (at the depths of 300–600 m). The proposed desalination system efficiency doubled over the conventional MED.

Mathematical and economic models of a low-temperature (LT) MED plant consisted of evacuated tube collector (ETC), storage tank, electrical heater, cooling unit, and flash tank were developed by Liu et al (2013). Increasing the steam temperature in the 1$^{st}$ effect led to a reduction in the size of the evaporator and freshwater cost, and increased the size of the storage tank. By increasing the number of effects, the size of the storage tank changed slightly, while, the size of the evaporator and desalination rate increased more.

Performance evaluation on a multi-effect distiller (capacity of 3 $m^3.d^{-1}$) including shell and tube HEX was carried out by Joo and Kwak (2013). The main parameter related to the performance of MED was the hot water flow rate. The PR of modified MED was about 2 and its desalination rate was 7 times more than that of a SS.

An 18,000 $m^3.d^{-1}$ capacity MED plant with an energy requirement of 250 MW was investigated by Rezaei et al (2017). Different energy sources such as fossil fuels (coal, oil, and gas), combined cycle, pebble-bed modular reactor, and pressurized water reactor were used to produce electricity for the MED. The cost analysis indicated that the optimum plant is the one that is powered by the combined cycle. By consideration of costs and lifetimes of proposed energy sources, the combined cycle, pressurized water, and pebble-bed modular reactors were short-, medium-, and long- term strategies to generate electricity and to couple with MED.

-

-



**Glossary**

| | |
|---|---|
| **AD :** | Adsorption desalination |
| **AH-HDH :** | Air heated humidification-dehumidification |
| **BF :** | Backward Feed is introduced in the last effect while the steam is introduced in the first effect. |
| **BPE :** | Boiling point elevation |
| **BR :** | Brine recirculation |
| **BR-MSF :** | Brine recycled multi-stage flash |
| **CAOW :** | Close air/open water cycle |
| **CCGT :** | combined cycle gas turbine |
| **CCPP :** | Combined cycle power plant |
| **CCST :** | combined cycle steam turbine |
| **CFD :** | Computational fluid dynamics |

| | |
|---|---|
| **CSP :** | Concentrating solar power |
| **ED :** | Electrodialysis - Electrodialysis desalination process transports salt ions from one solution through ion-exchange membranes to another solution under the influence of an applied electric potential difference |
| **ER :** | Entrainment ratio |
| **ETC :** | Evacuated tube collector |
| **FF :** | Forward Feed - Both Feed and Steam are introduced in the first effect. |
| **FF-MEE :** | Forward Feed - Multi-Effect Evaporation |
| **FO :** | Forward osmosis |
| **FPC :** | Flat plate collector |
| **GOR :** | Gained output ratio. A measure of thermal energy consumed in a desalination process. Number of kilograms of distilled water produced per kilogram of steam consumed. |
| **GT :** | Gas turbine |
| **HEX :** | Heat exchanger |
| **HGT :** | Humidified gas turbines |
| **HRSG :** | Heat recovery steam generator |
| **LBT :** | Low brine temperature |
| **LT :** | Low-temperature |
| **LT–MEE–ABHP :** | Low-Temperature-Multiple Effect Evaporator -Absorption Heat Pum |
| **LT–MEE–EHP :** | Multiple-Effect-Evaporator-Ejector Heat Pump |
| **M :** | Simple Mixer |
| **MED :** | Multi-effect distillation |
| **MEE :** | Multi-effect evaporation |
| **MIGD :** | Million imperial gallons per day |
| **MSF :** | Multi-stage flash |
| **MVC :** | Mechanical vapor compression |
| **OACW :** | Open air/close water cycle |
| **OAOW :** | Open air/open water cycle |
| **ORC :** | Organic Rankine Cycle |
| **OT :** | Once through |
| **OT-MSF :** | Once through multi-stage flash |
| **P/CF :** | Parallel/cross feed -Feed is distributed equally to all effects and brine leaving each effect is fed to the subsequent effect. |
| **P/W :** | Power to Water ratio |
| **PCM :** | Phase change material |
| **PF :** | Parallel Feed - Fresh Feed is introduced in every effect and |

| | |
|---|---|
| | steam is introduced in the first effect. |
| **P-HEX :** | Plate type heat exchanger |
| **PR :** | Performance ratio |
| **PTC :** | Parabolic trough collector |
| **PV :** | Photovoltaic |
| **PVDF :** | Polyvinylidene fluoride |
| **RO :** | Reverse osmosis |
| **SAH :** | Solar air heater |
| **SEC :** | Specific Energy Consumption |
| **SFED :** | Siphon flash evaporation desalination |
| **SS :** | Solar still |
| **ST :** | Steam turbine |
| **STIG :** | Steam-injected gas turbine |
| **SWH :** | Solar water heater |
| **TBT :** | Top Brine Temperature Maximum temperature of the brine during desalination process (top brine temperature (TBT) is in the range of 90-110 °C.) |
| **TDS :** | Total dissolved solids |
| **TES :** | Thermal energy storage |
| **TVC :** | Thermal vapor compression |
| **VOF :** | Volume of fluid |
| **VP-HDH :** | Varied pressure humidification-dehumidification |
| **WH-HDH :** | Water heated humidification-dehumidification |
| **ZEDS :** | Zero-carbon emission desalination system |

**Bibliography**

Qiblawey H.M., Banat F. (2008). Solar thermal desalination technologies, *Desalination*, 220, 633–644. [Direct and indirect solar desalination systems are compared based on distillate production and cost].

Alpatova A., Alsaadi A. Ghaffour N. (2018). Boron evaporation in thermally-driven seawater desalination: Effect of temperature and operating conditions, *Hazard. Matter.*, 351, 224–231. [The volatilization of boron in MSF and thermal AGMD is investigated].

Mayor B. (2019). Growth patterns in mature desalination technologies and analogies with the energy field, *Desalination*, 457, 75–84. [MED, MSF and RO units upscaling is experimented and the logistic growth curves of the historical dynamics in technology deployment is analyzed].

Ayati E., Rahimi-Ahar Z., Hatamipour M.S., Ghalavand Y. (2019). Water productivity enhancement in variable pressure humidification dehumidification (HDH) desalination systems using heat pump, Appl. Therm. Eng., 160, 114114. [Heat pump is added to different variable pressure HDH systems to investigate the system performance].

Rahimi-Ahar Z., Hatamipour M.S., Ghalavand Y. (2018). Solar assisted modified variable pressure humidification-dehumidification desalination system, *Energy Convers. Manag.*, 162, 321–330. [Variable pressure HDH systems are compared based on GOR and desalination rate].

Su W., Fournier J., Lacarrière B., Le Corre O. (2019). A new energy analysis model of seawater desalination based on thermodynamics, *Energy Procedia*, 158, 5472–5478.

Choi S. (2017). Thermal type seawater desalination with barometric vacuum and solar energy, *Energy*, 141, 1332–1349. [The passive vacuum pipe based on the hydrostatic head used in solar desalination unit to decrease the SEC].

Elsharqawy M.H., Lienhard J.H., Zubair S.M., Govindan P.N. (2013). Separation of a vaporizable component under reduced pressure, US 8, 465, 006 B2. [The vacuum in humidifier and dehumidifier is produced by barometric head and the GOR of the system is calculated].

International Desalination Association (IDA), (2016-2017). *Desalination year book*, Water desalination report.

Shih H. (2005). Evaluating the technologies of thermal desalination using low-grade heat, *Desalination*, 182, 461–469. [This paper compares the effectiveness of thermal desalination systems based on the thermal efficiency and performance ratio].

Malik S.N., Bahri P.A., Vu L.T.T. (2016). Steady state optimization of design and operation of desalination systems using Aspen Custom Modeler, *Comput. Chem. Eng*., 91, 247–256. [MSF, RO and MSF/RO units are optimized through Aspen Costum Modeller].

Bundschuh J., Ghaffour N., Mahmoudi H., Goosen M., Mushtaq S., Hoinkis J. (2015). Low-cost low-enthalpy geothermal heat for freshwater production: Innovative applications using thermal desalination processes, Renew. Sustain. *Energy Rev*., 43, 196–206. [The potential of using geothermal energy for powering the thermal-based desalination systems is explored].

Pouyfaucon A.B., García-Rodríguez L. (2018). Solar thermal-powered desalination: A viable solution for a potential market, *Desalination*, 435, 60–69. [An assessment of solar thermal-powered desalination technologies uses to identify the key issues for developing market opportunities].

Villacorte L.O. (2014). Algal Blooms and Membrane Based Desalination Technology, PhD thesis, Delft, Netherlands.

Ahmadvand S., Abbasi B., Azarfar B., Elhashimi M. (2019). Looking beyond energy efficiency: an applied review of water desalination technologies and an introduction to capillary-driven desalination, *Water*, 11, 696–726, 2019. [This paper reviews the desalination strategies with emphasis on means of using low-grade energy].

Villacorte L.O., Tabatabai S.A.A., Dhakal N., Amy G., Schippers J.C., Kennedy M.D. (2014). Algal Blooms: An Emerging Threat to Seawater Reverse Osmosis Desalination, *Desalin. Water Treat*., 55, 2601–2611.

Choon Ng K., Thu K., Oh S.J., Ang L., Shahzad M.W., Bin Ismail A. (2015). Recent developments in thermally-driven seawater desalination: Energy efficiency improvement by hybridization of the MED and AD cycles, *Desalination*, 356, 255–270. [A new isotherm model is developed based on energy distribution function for the MEDAD cycle to analyze the system thermodynamically].

Bandi C.S., Uppaluri R., Kumar A. (2016). Global optimization of MSF seawater desalination processes, *Desalination*, 394, 30–43. [The optimal design of MSF-M and MSF-BR processes is through Differential evolution algorithm].

Tanvir M.S., Mujtaba I.M. (2006). Neural network based correlations for estimating temperature elevation for seawater in MSF desalination process, *Desalination*, 195, 251–272. [Several neural networks based correlations use to predict TBT in MSF process].

Al-Weshahi M.A., Tian G., Anderson A. (2014). Performance enhancement of MSF desalination by recovering stage heat from distillate water using internal heat exchanger, 6th International Conference on Applied Energy, 61, 381–384.

Compain P. (2012). Solar energy for water desalination, *Procedia Eng*., 46, 220–227. [A review of MSF, MED and RO technologies based on cost comparison is reported].

Al-Hamahmy M., Fath H.E.S., Khanafer K. (2016). Techno-economical simulation and study of a novel MSF desalination process, *Desalination*, 386, 1–12. [An iterative mathematical model is developed to simulate MSF-BR to estimate the desalination rate and GOR].

Hawaidi E.A.M., Mujtaba I.M. (2010). Simulation and optimization of MSF desalination process for fixed freshwater demand: Impact of brine heater fouling, *Chem. Eng. J.*, 165, 545–553. [The brine heater fouling factor with variation of seawater temperature is studied in an MSF process].

Hanshik C., Jeong H., Jeong K., Choi S. (2016). Improved productivity of the MSF (multi-stage flashing) desalination plant by increasing the TBT (top brine temperature), *Energy*, 107, 683–692. [The effect of TBT on an MSF process is studied theoretically].

Hamed O.A., Al-Otaibi H.A. (2010). Prospects of operation of MSF desalination plants at high TBT and low antiscalant dosing rate, *Desalination*, 256, 181–189. [Scale formation using three types of antiscalants in an MSF is studied].

Nigim T.H., Eaton J.A. (2017). CFD prediction of the flashing processes in a MSF desalination chamber, *Desalination*, 420, 258–272. [CFD model for the flashing process inside a flashing chamber is developed through a two-phase VOF formulation].

Al-Othman A., Tawalbeh M., El Haj Assad M., Alkayyali T., Eisa A. (2018). Novel multi-stage flash (MSF) desalination plant driven by parabolic trough collectors and a solar pond: A simulation study in UAE, *Desalination*, 443, 237–244. [Solar assisted MSF system simulated through ASPEN HYSYS].

Darawsheh I., Islam M.D., Banat F. (2019). Experimental characterization of a solar powered MSF desalination process performance, *Therm. Sci. Eng. Prog.*, 10, 154–162 [Parametric study is carried out to optimize the MSF performance and cost].

Alsehli M., Choi J., Aljuhan M. (2017). A novel design for a solar powered multistage flash desalination, *Sol. Energy*, 153, 348–359. [An MSF system using concentrating solar collectors and thermal storage tank is developed].

Mabrouk A.A. (2013). Techno-economic analysis of tube bundle orientation for high capacity brine recycle MSF desalination plants, *Desalination*, 320, 24–32.

Messineo A., Marchese F. (2008). Performance evaluation of hybrid RO/MEE systems powered by a WTE plant, *Desalination*, 229, 82–93. [Thermal energy is recovered by a WTE plant to power an RO/MEE unit].

Halil İ., Söylemez M.S. (2012). Design and computer simulation on multi-effect evaporation seawater desalination system using hybrid renewable energy sources in Turkey, *Desalination*, 291, 23–40. [MEE-FF system using a flat plate collector and wind turbine are studied].

Khademi M.H., Rahimpour M.R., Jahanmiri A. (2009). Simulation and optimization of a six-effect evaporator in a desalination process, *Chem. Eng. Process: Process Intensification*, 48, 339–347. [A six-effect evaporator is optimized in terms of desalination rate and GOR].

Mittelman G., Kribus A., Mouchtar O., Dayan A. (2009). Water desalination with concentrating photovoltaic/thermal (CPVT) systems, *Sol. Energy*, 83, 1322–1334. [A photovoltaic/thermal collector coupled to a MEE plant is simulated to compute the production of electricity and water].

Piacentino A., Cardona E. (2010). Advanced energetics of a Multiple-Effects-Evaporation (MEE) desalination plant. Part II: Potential of the cost formation process and prospects for energy saving by process integration, *Desalination*, 259, 44–52. [A 6-effects MEE plant is optimized through application of the thermoeconomic productive structure].

Shen S., Guo Y., Gong L. (2018). Analysis of heat transfer critical point in LT-MEE desalination plant, *Desalination*, 432, 64–71. [Thermodynamic and structure parameters of an LT-MEE plant are analyzed].

Elsayed M.L., Mesalhy O., Mohammed R.H., Chow L.C. (2018a). Transient performance of MED processes with different feed configurations, *Desalination*, 438, 37–53. [BF, FF, PF and P/CF configurations of MED process are modelled under transient operation].

Elsayed M.L., Mesalhy O., Mohammed R.H., Chow L. C. (2018b). Exergy and thermo-economic analysis for MED-TVC desalination systems, *Desalination*, 447, 29–4. [BF, FF, PF and P/CF configurations of MED-TVC process are studied based on thermo-economic analysis].

Shahzad M.W., Burhan M., Gha N., Ng K.C. (2018). A multi evaporator desalination system operated with thermocline energy for future sustainability, *Desalination*, 435, 268–277. [The sustainability of desalination plants in future is investigated].

Liu X., Chen W., Gu M., Shen S., Cao G. (2013). Thermal and economic analyses of solar desalination system with evacuated tube collectors, *Sol. Energy*, 93, 144–150.

Joo H., Kwak H. (2013). Performance evaluation of multi-effect distiller for optimized solar thermal desalination, *Appl. Therm. Eng.*, 61, 491–499. [A performance evaluation on a multi-effect distiller is optimized based on mechanical and economical efficiencies].

Rezaei A., Naserbeagi A., Alahyarizadeh G., Aghaie M. (2017). Economic evaluation of Qeshm island MED-desalination plant coupling with different energy sources including fossils and nuclear power plants, *Desalination*, 422, 101–112. [The Qeshm island desalination plant using different energy sources is economically evaluated through a Desalination Economic Evaluation Program package].

Bonanos A. M. (2017). Physical modeling of thermo-compressor for desalination applications, *Desalination*, 412, 13–19. [A new model for thermocompressors of desalination plants based on compressible flow theory is developed].

Shen J., Xing Z., Wang X., He Z. (2014). Analysis of a single-effect mechanical vapor compression desalination system using water injected twin screw compressors, *Desalination*, 333, 146–153. [This paper analyses the performance of a single-effect MVC system using water injected twin screw compressors].

He W.F., Ji C., Han D., Wu Y.K., Huang L., Zhang X.K. (2017). Performance analysis of the mechanical vapor compression desalination system driven by an organic Rankine cycle, *Energy*, 141, 1177–1186. [An MVC plant coupling with an organic Rankine cycle is proposed].

Bin Amer A.O. (2009). Development and optimization of ME-TVC desalination system, *Desalination*, 249, 1315–1331. [A steady state mathematical model of the ME-TVC desalination system is developed using Engineering Equations Solver to evaluate the system performance].

Alasfour F.N., Bin Amer A.O. (2006). The feasibility of integrating ME-TVC + MEE with Azzour South Power Plant: Economic evaluation, *Desalination*, 197, 33–49. [The cost analysis of the ME-TVC-MEE plant in Azzour is reported].

Chen L., Xu Q., Gossage J.L., Lou H.H. (2016). Simulation and economic evaluation of a coupled thermal vapor compression desalination process for produced water management, *J. Nat. Gas Sci. Eng.*, 36, 442–453. [A TVC desalination plant powered by flare gas is simulated in Aspen Plus].

Yildirim C., Solmuş I. (2014). A parametric study on a humidification-dehumidification (HDH) desalination unit powered by solar air and water heaters, *Energy Convers. Manag.*, 86, 568–575. [The parametric study of a solar assisted HDH system is reported].

Lienhard J.H., Thiel G.P., D. Warsinger D.M., Banchik L.D. (2016). Low carbon desalination: status and research, development, and demonstration needs, Report of a Workshop, Massachusetts Institute of Technology in Association with the Global Clean Water Desalination Alliance.

Narayan G.P., Sharqawy M.H., Summers E.K., Lienhard J.H., Zubair S.M., Antar M.A. (2010). The potential of solar-driven humidification-dehumidification desalination for small-scale decentralized water production, Renew. *Sustain. Energy Rev.*, 14, 1187–1201. [This paper provides a comprehensive review of HDH desalination systems].

Yamali C. (2007). Theoretical investigation of a humidification-dehumidification desalination system configured by a double-pass flat plate solar air heater, *Desalination*, 205, 163–177. [A double-pass solar air heater is used in HDH system to improve the system performance].

Bourouni K., Martin R., Tadrist L., Chaibi M.T. (1999). Heat transfer and evaporation in geothermal desalination units, *Appl. Energy*, 64, 129–147.

He W.F., Han D., Zhu W.P., Ji C. (2018). Thermo-economic analysis of a water-heated humidification-dehumidification desalination system with waste heat recovery, *Energy Convers. Manag.*, 160, 182–190. [Water heated HDH system using waste heat is analyzed thermo-economically].

Giwa A., Fath H., Hasan S.W. (2016). Humidification-dehumidification desalination process driven by photovoltaic thermal energy recovery (PV-HDH) for small-scale sustainable water and power production, *Desalination*, 377, 163–171. [PV-HDH system as a co-generation plant is investigated].

Rahimi-Ahar Z., Hatamipour M.S., Ghalavand Y. (2018). Experimental investigation of a solar vacuum humidification-dehumidification (VHDH) desalination system, *Desalination*, 437, 73–80. [VHDH desalination system is optimized using response surface methodology].

Rahimi-Ahar Z., Hatamipour M.S., Ghalavand Y., Palizvan A. (2020). Comprehensive Study on Vacuum Humidification-Dehumidification (VHDH) Desalination, *Appl. Therm. Eng.*, 169, 114944. [Exergy analysis on VHDH desalination system is revealed].

Ghalavand Y., Hatamipour M. S., Rahimi A. (2014). Humidification compression desalination, *Desalination*, 341,120–125. [HC is introduced as a highly efficient HDH system compared to conventional air and water heated HDH system].

Ghalavand Y., Rahimi A., Hatamipour M.S. (2018). Mathematical modeling for humidifier performance in a compression desalination system: Insulation effects, *Desalination*, 433, 48–55. [The effect of humidifier insolation on HC performance is revealed].

Zhang Y., Zhu C., Zhang H., Zheng W., You S. (2018). Experimental study of a humidification-dehumidification desalination system with heat pump unit, *Desalination*, 442, 108–117. [A heat pump is coupled to an HDH system to improve dehumidification efficiency].

Ghaffour N., Bundschuh J., Mahmoudi H., Goosen M.F.A. (2015). Renewable energy-driven desalination technologies: A comprehensive review on challenges and potential applications of integrated systems, *Desalination*, 356, 94–114. [The general water background, renewable energy status and the potential of renewable energy assisted desalination systems in Iran are reviewed].

Choon Ng K., Thu K., Kim Y., Chakraborty A., Amy G. (2013). Adsorption desalination: An emerging low-cost thermal desalination method, *Desalination*, 308, 161–179. [An adsorption desalination system using waste heat is developed to prove as an emerging and low cost method].

Shahzad M.W., Choon Ng K., Thu K., Baran B. (2014). Multi effect desalination and adsorption desalination (MEDAD): A hybrid desalination method, *Appl. Therm. Eng.*, 72, 289–297. [MEDAD system is introduced as an advanced desalination plant].

Shahzad M.W., Thu K., Kim Y., Choon Ng K. (2015). An experimental investigation on MEDAD hybrid desalination cycle, *Appl. Energy*, 148, 273–281. [The productivity and scale formation are experimentally investigated in an MEDAD desalination system].

Choon Ng K., Thu K., Jin S., Ang L., Shahzad M.W., Bin A. (2015). Recent developments in thermally-driven seawater desalination: Energy efficiency improvement by hybridization of the MED and AD cycles, *Desalination*, 356, 255–270. [Energy efficiency of an MEDAD desalination system is revealed].

Kim Y., Thu K., Choon Ng K., Amy G.L., Ghaffour N. (2016). A novel integrated thermal- / membrane-based solar energy-driven hybrid desalination system: Concept description and simulation results, *Water Res*., 100, 7–19.

Sadri S., Khoshkhoo R.H., Ameri M. (2018). Optimum exergoeconomic modeling of novel hybrid desalination system (MEDAD+RO), *Energy*, 149, 74–83. [MEDAD-RO plant is exergo-economically optimized].

Belessiotis V., Kalogirou S., Delyannis E. (2016). *Thermal Solar Desalination, Methods and Systems*, Elsevier. [Different thermal based desalination plants are comprehensively studied].

Lawson K.W., Lioyd D.R. (1997) Membrane distillation, *Membr. Science*, 124, 1–25.

Burhan M., Shahzad M.W., Ybyraiymkul D., Oh S.J., Gha N., Ng K.C. (2019). Performance investigation of MEMSYS vacuum membrane distillation system in single effect and multi-effect mode, *Sustain. Energy Technol. Assessments*, 34, 9–15.

Cheng D., Li N., Zhang J. (2018). Modeling and multi-objective optimization of vacuum membrane distillation for enhancement of water productivity and thermal efficiency in desalination, *Chem. Eng. Res.* Dec. 2018, 2, 697–713. [The multi-objective modeling and optimization in the vacuum membrane distillation are performed through response surface methodology and desirability function approach].

Adham S., Hussain A., Matar J.M., Dores R., Janson A. (2013). Application of Membrane Distillation for desalting brines from thermal desalination plants, *Desalination*, 314, 101–108. [The feasibility of MD to desalinate brine from thermal plants is evaluated].

Kumar P.V., Kumar A., Prakash O., Kaviti A.K. (2015). Solar stills system design: A review, Renew. *Sustain. Energy Rev*., 51, 153–181. [Different solar stills are reviewed].

Jani H.K., Modi K.V. (2018). A review on numerous means of enhancing heat transfer rate in solar-thermal based desalination devices, Renew. *Sustain. Energy Rev*., 93, 302–317. [Solar-thermal desalination systems are reviewed based on heat transfer rate enhancement prospect].

Sharshir S.W., Ellakany Y.M., Algazzar A.M., Elsheikh A.H., Elkadeem M.R., Edreis E.M.A., Waly A.S., Sathyamurthy R., Panchal H., Elashry M.S. (2019). A mini review of techniques used to improve the tubular solar still performance for solar water desalination, *Process Saf. Environ. Prot*., 124, 204–212. [Tubular solar sills are reviewed].

Li C., Goswami Y., Stefanakos E., (2013). Solar assisted seawater desalination: A review, Renew. *Sustain. Energy Rev*., 19, 136–163. [A detailed review on solar desalination plants is revealed].

Chandrashekara M., Yadav A. (2017). Water desalination system using solar heat: A review, Renew. *Sustain. Energy Rev*., 67, 1308–1330. [Solar desalination plants are reviewed].

Rashidi S., Abolfazli J., Rahbar N. (2017). Partitioning of solar still for performance recovery: Experimental and numerical investigations with cost analysis, *Sol. Energy*, 153, 41–50. [The effects of partitioning in solar still on energy recovery are investigated].

Kumar S., Dubey A., Tiwari G.N. (2014). A solar still augmented with an evacuated tube collector in forced mode, *Desalination*, 347, 15–24. [A modified solar still coupled to an evacuated tube collector in forced mode is optimized].

Sriram V., Samuel Hansen R., Kalidasa Murugavel K. (2013). Experimental study of a low pressure solar still, *Appl. Sol. Energy*, 49, 137–141. [A low pressure, single basin double slope solar still by various wick and porous materials is tested].

Singh D.B, Al-Helal I.M. (2018). Energy metrics analysis of N identical evacuated tubular collectors integrated double slope solar still, *Desalination*, 432, 10–22. [A double slope solar still integrated with N identical evacuated tubular collectors is analyzed based on energy metrics].

Dahdah H., Mitsos A. (2014). Structural optimization of seawater desalination: I. A flexible superstructure and novel MED-MSF configurations, *Desalination*, 344, 252–265.

Nasser A., Fath H. E. S. (2015). Technoeconomic study of a novel integrated thermal MSF–MED desalination technology, *Desalination*, 371, 115–125. [An MSF-MED plant is analyzed thermo-economically].

Cardona E., Culotta S., Piacentino A. (2002). Energy saving with MSF-RO series desalination plants, *Desalination*, 153, 167–171. [MSF-RO hybrid plant is introduced as an energy saving plant compared to single desalination unit.

Helal A.M., El-Nashar A.M., Al-Katheeri E.S., Al-Malek S.A. (2004). Optimal design of hybrid RO/MSF desalination plants Part II: Results and discussion, *Desalination*, 160, 13–27. [A hybrid RO/MSF plant is optimized based on minimum water cost].

Loutatidou S., Arafat H.A. (2015). Techno-economic analysis of MED and RO desalination powered by low-enthalpy geothermal energy, *Desalination* 365, 277–292.

Khoshgoftar Manesh M.H., Ghalami H., Amidpour M., Hamedi M.H. (2013). Optimal coupling of site utility steam network with MED-RO desalination through total site analysis and exergoeconomic optimization, *Desalination*, 316, 42–52. [New procedure for optimal coupling MED-RO and steam network is presented].

Altaee A., Mabrouk A., Bourouni K., Palenzuela P. (2014). Forward osmosis pretreatment of seawater to thermal desalination: High temperature FO-MSF/MED hybrid system, *Desalination*, 339, 18–25. [Forward osmosis seawater pretreatment is proposed for the removal of scale ions from seawater to the thermal desalination plants].

Altaee A., Zaragoza G.A. (2014). A conceptual design of low fouling and high recovery FO–MSF desalination plant, *Desalination*, 343, 2–7. [Forward osmosis is suggested for seawater pretreatment to the MSF process].

El-Dessouky H., Ettouney H., Al-Fulaij H., Mandani F. (2000). Multistage flash desalination combined with thermal vapor compression, *Chem. Eng. Process.*, 39, 343–356. [The performance of an MSF-TVC desalination system is analyzed].

Khalid K.A., Antar M.A., Khalifa A., Hamed O.A. (2018). Allocation of thermal vapor compressor in multi-effect desalination systems with different feed configurations, *Desalination*, 426, 164–173. [An MED-TVC is analyzed to extract the portion of the formed vapor in an effect and mix it with motive steam].

Cipollina A., Agnello M., Piacentino A., Tamburini A., Ortega B., Palenzuela P., Alarcon D., Micale G. (2017). A dynamic model for MED-TVC transient operation, *Desalination*, 413, 234–257. [An MED-TVC palnt is modelled in transient operation through gPROMS].

Hanafi A.S., Mostafa G.M., Waheed A., Fathy A. (2015). 1-D Mathematical Modeling and CFD Investigation on Supersonic Steam Ejector in MED-TVC, *Energy Procedia*, 75, 3239–3252.

Gu W., Wang X., Wang L., Yin X., Liu H. (2019). Performance investigation of an auto-tuning area ratio ejector for MED-TVC desalination system, *Appl. Therm. Eng.*, 155, 470–479. [An auto-tuning area ratio ejector is equipped to enhance the performance of MED-TVC desalination system].

Sagharichiha M., Jafarian A., Asgari M., Kouhikamali R. (2014). Simulation of a forward feed multiple effect desalination plant with vertical tube evaporators, *Chem. Eng. Process. Process Intensif.*, 75, 110–118.

Wang C., Wang L., Wang X., Zhao H. (2017). Design and numerical investigation of an adaptive nozzle exit position ejector in multi-effect distillation desalination system, *Energy*, 140, 673–681. [An adaptive nozzle exit position ejector

is proposed to enhance ejector performance in MED system].

Al-Mutaz I.S., Wazeer I. (2014). Development of a steady-state mathematical model for MEE-TVC desalination plants, *Desalination*, 351, 9–18. [A steady-state model of MEE-TVC system and its solution procedure are developed].

Abdelkarrim M.L.E. (2019). Dynamic behavior and performance of different types of multi-effect desalination plants, PhD thsis, Central Florida Orlando, Florida. [Different configurations of MEE-TVC plants are studied under transient operation].

Farshchi F., Khosravi M., Shirzaei I. (2016). Experimental study of a cascade solar still coupled with a humidification-dehumidification system, *Energy Convers. Manag.*, 115, 80–88. [A cascade solar still is coupled to an HDH system to improve the system performance].

Sharshir S.W., Peng G., Yang N., Eltawil M.A., Ali M.K.A., Kabeel A.E. (2016a). A hybrid desalination system using humidification-dehumidification and solar stills integrated with evacuated solar water heater, *Energy Convers. Manag*., 124, 287–296. [The performance of a hybrid HDH-SS is evaluated].

Sharshir S.W., El-Samadony M.O.A., Peng G., Yang N., Essa F.A., Hamed M.H., Kabeel A.E. (2016b). Performance enhancement of wick solar still using rejected water from humidification-dehumidification unit and film cooling, *Appl. Therm. Eng*., 108, 1268–127. [A wick solar still is coupled to an HDH system to improve the system performance].

Mays L. W. (2007). *Water resources sustainability*, New York: McGraw-Hill, 363.6 M3.

Burbano, A., Brankhuber P. (2012). Demonstration of Membrane Zero Liquid Discharge for Drinking Water Systems-A Literature Review, WERF5T10a. Water Environment Research Foundation: Alexandria, VA.

Nakoa K., Rahaoui K., Date A., Akbarzadeh A. (2016). Sustainable zero liquid discharge desalination (SZLDD), *Sol. Energy*, 135, 337–3476. [A sustainable SZLDD is developed by coupling a direct contact membrane distillation unit and a solar pond].

Cabassud C., Mericq J., (2010). Vacuum membrane distillation of seawater reverse osmosis brines, *Sol. Energy*, 44, 2010.

Liu J., Wang L., Jia L., Wang X. (2017). The influence of the area ratio on ejector efficiencies in the MED-TVC desalination system, *Desalination*, 413, 168–175. [CFD is used to investigate the effect of the area ratio on ejector efficiencies in MED-TVC desalination plant].

Helal A.M. (2009). Hybridization-a new trend in desalination, *Desalin. Water Reuse*, 3, 120–135.

Agashichev S.P. (2004). Analysis of integrated co-generative schemepresent value of expenses and levelized cost of water, *Desalination*, 164, 281–302.

Shahzad M.W., Burhan M., Ybyraiymkul D., Choon Ng K.. (2019). Desalination Processes: Efficiency and Future Roadmap, *Entropy*, 21, 84–98. [A standard universal performance ratio-based evaluation method is proposed to evaluate the desalination system efficiency].

Hamed O.A. (2016). Thermoeconomic analysis of combined power cycle integrated with MSF/SWRO desalination plant, *Desalin. Water Treat.*, 3994, 1–10.

Afgan N.H., Darwish M., Carvalho M.G. (1999). Sustainability assessment of desalination plants for water, *Desalination*, 124, 19–31.

Shahzad M.W., Burhan M., Choon Ng K.. (2019). A standard primary energy approach for comparing desalination processes, npj Clean Water, 2, 1–7. [A standard primary energy-based thermodynamic framework is presented to address the energy efficacy of assorted desalination processes].

Al-Sofi M.A., Hassan A.M., El-Sayed, E.E. (1992). Integrated and nonintegrated Plants, Power/MSF/RO plants, *Int. Desalin. Water Reuse*, 2, 10–16.

Wang Y., Lior N. (2007). Fuel allocation in a combined steam-injected gas turbine and thermal seawater desalination system, *Desalination*, 214, 306–326.

Mussati S.F., Aguirre P.A., Scenna N.J. (2005). Optimization of alternative structures of integrated power and desalination plants, *Desalination*, 182, 123–129.

Gadhamshetty V., Gnaneswar V., Nirmalakhandan N. (2014). Thermal energy storage system for energy conservation and water desalination in power plants, *Energy*, 66, 938–949. [A novel application of a sensible thermal energy storage system for energy conservation and water desalination in power plants is revealed].

Zuo L., Ding L., Chen J., Liu Z., Qu N., Zhou X., Yuan Y. (2018). The effect of different structural parameters on wind supercharged solar chimney power plant combined with seawater desalination, *Energy Convers. Manag*., 176, 372–383.

Wade N.M. (1999). Energy and cost allocation in dual-purpose power and desalination plants, *Desalination*, 123, 115–125. [This paper reviews energy and cost allocation methods applicable to dual-purpose power and desalination plants].

Wang Y., Lior N. (2006). Performance analysis of combined humidified gas turbine power generation and multi-effect thermal vapor compression desalination systems- Part 1: The desalination unit and its combination with a steam-injected gas turbine power system, *Desalination*, 196, 84–1046. [A hybrid power and water system based on the evaporative gas turbine is studied].

Mokhtari H., Sepahvand M. (2016.) Thermoeconomic and exergy analysis in using hybrid systems (GT + MED + RO) for desalination of brackish water in Persian Gulf, *Desalination*, 399, 1–15.

Gude V.G. (2018). Use of exergy tools in renewable energy driven desalination systems, *Therm. Sci. Eng. Prog*., 8, 154–170. [This paper elaborates on use of exergy tools to evaluate renewable energy driven desalination processes to evaluate their thermodynamic efficiency].

Aberuee M.J., Baniasadi E., Ziaei-Rad M. (2017). Performance analysis of an integrated solar based thermo-electric and desalination system, *Appl. Therm. Eng.*, 110, 399–411. [The irreversibility of a solar thermo-electric and desalination plant is minimized using genetic algorithm].

Al-Weshahi M.A., Anderson A., Tian G. (2013). Exergy efficiency enhancement of MSF desalination by heat recovery from hot distillate water stages, *Appl. Therm. Eng.*, 53, 226–233. [The exergy efficiency of an MSF system is calculated using IPSEpro software].

Nafey A.S., Fath H.E.S., Mabrouk A.A. (2006). Thermo-economic investigation of multi effect evaporation (MEE) and hybrid multi effect evaporation-multi stage flash (MEE-MSF) systems, *Desalination*, 201, 241–254. [MEE and MEE-MSF systems are compared based on thermo-economic analysis].

Jamil M.A., Zubair S.M. (2017). Design and analysis of a forward feed multi-effect mechanical vapor compression desalination system: An exergo-economic approach, *Energy*, 140, 1107–1120. [An exergo-economic analysis of a forward-feed MEMVC desalination system is performed].

Han D., He W.F., Yue C., Pu W.H. (2017). Study on desalination of zero-emission system based on mechanical vapor compression, *Appl. Energy*, 185, 1490–1496. [Performance of the single stage and double stage ZEDS is calculated].

Khalilzadeh S., Hossein Nezhad A.H. (2018). Utilization of waste heat of a high-capacity wind turbine in multi-effect distillation desalination: Energy, exergy and thermoeconomic analysis, *Desalination*, 439, 119–137. [MED system using waste heat is analyzed thermo-economically].

Elsayed M.L., Mesalhy O., Mohammed R.H., Chow L.C. (2019). Transient and thermo-economic analysis of MED-MVC desalination system, *Energy*, 167, 283–296. [An MED-MVC plant is analyzed thermo-economically under transient operation].

Yousef M.S., Hassan H., Ahmed M., Ookawara S. (2017). Energy and exergy analysis of single slope passive solar still under Egyptian climate conditions, *Energy Procedia*, 141, 18–23. [A single slope solar still is analyzed exergetically].

Layek A. (2018). Exergetic analysis of basin type solar still, *Eng. Sci. Technol*., 21, 99–106. [Basin type solar still is analyzed exergetically].

Asbik M., Ansari O., Bah A., Zari N., Mimet A., El-Ghetany H. (2016). Exergy analysis of solar desalination still combined with heat storage system using phase change material (PCM), *Desalination*, 381, 26–37. [The effect of PCM on solar still performance is investigated].

Sarhaddi F., Farshchi Tabrizi F., Aghaei Zoori H., Seyed Mousavi S.A.H. (2017). Comparative study of two weir type cascade solar stills with and without PCM storage using energy and exergy analysis, *Energy Convers. Manag*., 133, 97–109. [The effect of using PCM on energy and exergy efficiencies of two weir type cascade solar stills is clarified].

Aghaei Zoori H., Farshchi Tabrizi F., Sarhaddi F., Heshmatnezhad F. (2013). Comparison between energy and exergy efficiencies in a weir type cascade solar still, *Desalination*, 325, 113–121. [Energy and exergy efficiencies of a weir type cascade solar still are calculated].

Almutairi A., Pilidis P., Al-mutawa N. (2016). Energetic and exergetic analysis of cogeneration power combined cycle and ME-TVC-MED water desalination plant: Part-1 operation and performance, *Appl. Therm. Eng*., 103, 77–91. [CCPP-ME-TVC-MED co-generation plant is analyzed thermodynamically].

Almutairi A., Pilidis P., Al-Mutawa N. (2015). Energetic and exergetic analysis of combined cycle power plant: Part-1 Operation and Performance, *Energies*, 8, 14118–14135. [CCPP-ME-TVC-MED co-generation plant is analyzed using the thermodynamic properties of seawater].

Zhou S., Guo Y., Mu X., Shen S. (2015). Effect of design parameters on thermodynamic losses of the heat transfer process in LT-MEE desalination plant, *Desalination*, 375, 40–47. [Thermodynamic losses in an LT-MEE plant are investigated].

Brogioli D., La F., Yin N. (2018). Thermodynamic analysis and energy efficiency of thermal desalination processes, *Desalination*, 428, 29–39. [Thermodynamic study of MED and MSF plants are clarified their energy efficiencies].

Wang Y., Lior N. (2011). Thermoeconomic analysis of a low-temperature multi-effect thermal desalination system coupled with an absorption heat pump, *Energy*, 36, 3878–3887. [An LT-MEE desalination system coupled with an LiBre$H_2O$ absorption heat pump is analyzed thermo-economically].

Nafey A.S., Fath H.E.S., Mabrouk A.A. (2008). Thermoeconomic design of a multi-effect evaporation mechanical vapor compression (MEE-MVC) desalination process, *Desalination*, 230, 1–15. [MED-TVC process is optimized in term of GOR].

Zhou S., Gong L., Liu X., Shen S. (2019). Mathematical modeling and performance analysis for multi-effect evaporation/multi-effect evaporation with thermal vapor compression desalination system, *Appl. Therm. Eng*., 113759. [MEE and MEE-TVC using the industrial waste heat are compared based on GOR].

Alasfour F.N., Darwish M.A., Bin Amer A.O. (2005). Thermal analysis of ME-TVC+MEE desalination systems, *Desalination*, 174, 39–61. [Conventional ME-TVC, ME-TVC with regenerative feed heaters and ME-TVC coupled to a conventional MEE systems are studied exergetically].

Salimi M., Reyhani H.A., Amidpour M. (2018). Thermodynamic and economic optimization of multi-effect desalination unit integrated with utility steam network, *Desalination*, 427, 51–59. [The integration of an MED plant with utility steam network system is evaluated].

Alasfour F.N., Abdulrahim H.K. (2011). The effect of stage temperature drop on MVC thermal performance, *Desalination*, 265, 213–221. [Steady state hybrid MSF–MVC system is modelled to study the parametrically].

Packiaraj V.S., Velraj R., Jalihal P. (2018). Transient analysis of steam accumulator integrated with solar based MED-TVC system, *Desalination*, 435, 3–22. [Solar assisted MED-TVC system is designed using a buffer storage system].

Samake O, Galanis N, Sorin M. (2018). Thermo-economic analysis of a multiple-effect desalination system with ejector vapour compression, *Energy*, 144, 1037–1051. [FF and P/CF configurations are modeled exergo-economically based on the SPECO method].

Ahmad M., Zubair S.M. (2018). Effect of feed flow arrangement and number of evaporators on the performance of multi-effect mechanical vapor compression desalination systems, *Desalination*, 429, 76–87. [FF, PF and P/CF configurations of a multi-effect mechanical vapor compression are compared based on energy consumption, exergy destruction, heat transfer area and production cost].

Farsi A., Dincer I. (2019). Development and evaluation of an integrated MED/membrane desalination system, *Desalination*, 463, 55–68. [The entropy generation and GOR of MED and DCMD are revealed through solving the energy, entropy and exergy balance equations].

Aguirre N.J.S., Scenna P.A. (1989). Optimal thermodynamic synthesis of dual-purpose desalination plants, *Chem. Eng. Sci.*, 44, 283–296.

**Biographical Sketches**

**Zohreh Rahimi-Ahar** obtained her PhD degree in chemical engineering from university of Isfahan on Oct. 2018. Her activities focused on the experimental studies of humidification-dehumidification (HDH) desalination systems and development of process simulation and modelling. She is continuing her researches in thermal desalination systems during her postdoctoral course in university of Isfahan. With combination of these investigations, she aims to gain comprehensive understanding for the chances of thermal water desalination systems development.

**Mohammad Sadegh Hatamipour**, PhD, is a full time professor with educational and research duties in chemical engineering department of university of Isfahan, Isfahan, Iran. He obtained his BS, Ms and PhD degrees in Chemical engineering from Shiraz University. He has more than 20 years on transport phenomena projects, including drying, gas absorption, environmental protection, heat recovery and solar energy. His works focuses specifically on the HDH water desalination research projects in the last 5 years.